Atomic Radiative and Radiationless Yields for *K* and *L* Shells

M. O. Krause

Transuranium Research Laboratory, Oak Ridge National Laboratory, Oak Ridge, Tennessee 37830, USA

The available body of information on (a) fluorescence, Auger, and Coster-Kronig yields, (b) radiative and radiationless transition rates, (c) level widths, (d) x-ray and Auger line widths, (e) x-ray and Auger spectra, and (f) Coster-Kronig energies has been used to generate an internally consistent set of values of atomic radiative and radiationless yields for the K shell ($5 \le Z \le 110$) and the L subshells ($12 \le Z \le 110$). Values of fluorescence yields ω_K, ω_1, ω_2, ω_3, Coster-Kronig yields f_1, $f_{1,2}$, $f_{1,3}$, $f'_{1,3}$, $f_{2,3}$, Auger yields a_K, a_1, a_2, a_3, and effective fluoresence yields ν_1 and ν_2 are presented in tables and graphs. Estimates of uncertainties are given. Updated and expanded graphs of partial and total widths of K, L_1, L_2, and L_3 levels are presented as well as a reference list of papers published since about 1972.

Key words: Atomic properties; Auger yield; Coster-Kronig yield; effective fluorescence yield; fluorescence yield; K shell; L shell; non-radiative yield; partial level width; radiative yield.

Contents

Nomenclature

Previous convention is followed that omits the L shell designation in subscripts, for example, ω_1 instead of ω_{L_1}.

S	Transition rate.
S_j (j = R,A,C)	Transition rates of radiative (R), Auger (A) and Coster-Kronig (C) components.
Γ	Natural level width.
Γ_j (j = R,A,C)	Partial level widths: radiative width (R), Auger width (A), and Coster-Kronig width (C).
ω_i (i = K,1,2,3)	Fluorescence or radiative yield of K, L_1, L_2, L_3 levels.
a_i (i = K,1,2,3)	Auger yield of K, L_1, L_2, L_3 levels
$f_1 = f_{1,2} + f_{1,3}$	Coster-Kronig yield of L_1 level
$f_{i,k}$ (i,k = 1,2: 1,3; 2,3)	Coster-Kronig yield for radiationless transitions between L levels i,k

0047-2689/79/020307-21/$04.00

$f'_{1,3}$ Intrashell radiative yield for transition $L_1 \rightarrow L_3$.

ν_1, ν_2 Effective fluorescence yield of L_1 and L_2 levels.

Z Atomic number.

1. Introduction

Although K shell fluorescence yields have been reviewed on several occasions [1–3][1], no evaluation has been made of the radiative and radiationless yields of the L subshells of the elements. Previously, an attempt to systematize L shell yields was made by Listengarten [4], who presented semi-empirical values for $Z > 45$. An analytical expression for the L_3 fluorescence yield, ω_3, has been reported by Burhop and Asaad [3], and least-squares-fits to experimental ω_2 and ω_3 data for $Z > 47$ were made by Fink and Rao [5].

In this work, sets of values that are mutually consistent and compatible with the available body of information on yields and related quantities were generated for fluorescence, Coster-Kronig, and Auger yields. For the K shell, previous sets of recommended values [2,3] were augmented by recent data[2] and extended beyond $Z = 93$ to $Z = 110$; for the L shell, the evaluation was based on original experimental and theoretical results and covers the range from $Z = 12$ to $Z = 110$. Adopted values pertain to singly ionized atoms with the qualification that the evaluation utilized, along with free-atom single-hole theoretical data, experimental data that usually contain contributions from solid state, chemical and multiple-ionization effects. However, these contributions, which have rarely been delineated in past work, supposedly have a very small effect [6] on the yields except in the light elements and at onsets and cutoffs of Coster-Kronig transitions.

Tables and graphs provide the best yield values that can presently be given on the basis of all pertinent data; such values are essential in the areas of basic and applied sciences concerned with innershell ionization phenomena.

2. Definitions and Relations

The lifetime τ of a single hole in a given level is related to the natural width Γ of that level by the uncertainty principle:

$$\Gamma\tau = \hbar \tag{1}$$

and because $S = 1/\tau$, where S is the rate for all processes filling the hole, we have

$$S = \Gamma/\hbar. \tag{2}$$

Assuming the different decay modes are independent, the total rate S will be given by the sum of the partial rates

$$S = S_R + S_A + S_C \tag{3}$$

and the total level width (natural width) by

$$\Gamma = \Gamma_R + \Gamma_A + \Gamma_C, \tag{4}$$

where subscripts denote the radiative, Auger, and Coster-Kronig branches. Yields for the various processes are defined as follows:

Radiative or fluorescence yield $\omega = \Gamma_R/\Gamma$ (5)

Auger yield $a = \Gamma_A/\Gamma$ (6)

Coster-Kronig yield $f = \Gamma_C/\Gamma$ (7)

The sum of radiative yield ω and radiationless yields a and f is unity:

$$\omega + a + f = 1. \tag{8}$$

Furthermore, the effective L-shell fluorescence yields ν_1 and ν_2 for an initial vacancy in the L_1 and L_2 subshells[3] are given, respectively, by

$$\nu_1 = \omega_1 + \omega_2 f_{1,2} + \omega_3(f_{1,3} + f_{1,2}f_{2,3} + f'_{1,3}) \tag{9}$$

and

$$\nu_2 = \omega_2 + \omega_3 f_{2,3} \tag{10}$$

in terms of the subshell fluorescence and Coster-Kronig yields and the intrashell radiative yield $f'_{1,3}$, which refers to the transition $L_1 \rightarrow L_3$.

The width of an x-ray line is given by

$$\Gamma(X \rightarrow Y) = \Gamma(X) + \Gamma(Y) \tag{11}$$

where X and Y are the levels involved in the transition.

Analogously, the width of an Auger or Coster-Kronig line is given by

$$\Gamma(X \rightarrow YZ) = \Gamma(X) + \Gamma(YZ) \tag{12}$$

where YZ is a double-hole configuration. Widths of eqs (11) and (12), or directly measured level widths Γ, can be correlated with transition rates S (eqs (2) to (4)), and yields (eqs (5) to (7)) only if (a) effects other than lifetime broadening are absent or negligible, and (b) the width of one of the levels involved in a transition is known or is small compared to the other.

[1] Figures in brackets indicate literature references at the end of this paper.

[2] These data are compiled in the Appendix.

[3] Designation for the L shell is dropped in subscripts.

3. Source Material

The following material was utilized in the evaluation:) experimental fluorescence, Auger, and Coster-Kronig elds, (b) theoretical radiative and non-radiative rates,) level widths, (d) x-ray and Auger-line widths, (e) x-ray nd Auger spectra, and (f) Coster-Kronig energies. riginal data of item (a) were taken from the compila- ons of references 2 and 3, and from later work ummarized in the Appendix, but excluding data from hose ion-atom collisions that produce highly ionizied pecies. Rates were taken from the graphs of partial evel widths displayed in figures 1 to 4. For level widths ecent data (Appendix) and compilations [7–9] were consulted, and for x-ray line widths recent evaluations [10,11] formed the major input. Most data on Auger line widths and x-ray spectra are of recent origin as is a comphrehensive calculation of Coster-Kronig energies [12]. Source material up to October, 1977 was considered.

4. Partial and Total Atomic Level Widths

Theoretical transition rates, expressed as partial level widths, are displayed in figures 1 to 4 to allow the reader to interrelate the different categories of source material, to assess the relative importance of the various quantities in different Z regions, and to visualize trends of rates, yields and level widths as a function of Z.

Figures 1 to 4 are updated and expanded versions of the K and L graphs of an earlier presentation [13] of theoretical results. Curves of partial widths Γ_A and Γ_C show averaged results for K shell [14] and L subshells [15] from the same sources used in reference 13; but in averaging, the hydrogenic-type calculations were given much less weight, especially at low Z, than previously [13]. In figures 2 and 3, discontinuities in the Γ_C plots were located in accordance with a recent calculation [12] of Coster-Kronig energies. Partial widths Γ_R were taken solely from relativistic Hartree-Fock calculations [16,17]. Relativistic Hartree-Slater values [18] were used, however, to aid in the interpolation of the relativistic Hartree-Fock values reported in references 16 and 17.

In the evaluation procedure outlined below, theoretical widths of the L subshells were modified to be compatible with experimental data of level and line widths. The resulting semi-empirical values, which contain many of the quantities used as source material (items (b) to (f) of sec. 3), are plotted in the insets of figures 2 and 3 in those regions in which substantial changes occur. In the

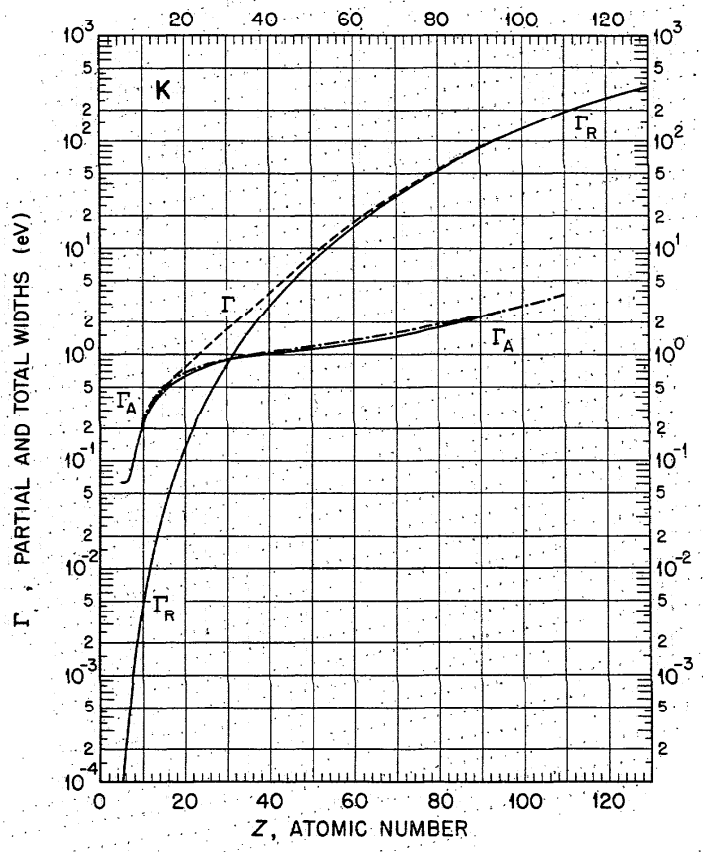

FIGURE 1. Theoretical partial and total atomic level widths for K shell. Γ_A = Auger width, Γ_R = radiative width, Γ = total width. Dot-dash curve represents semi-empirical Γ_A curve obtained from adopted ω_K values and theoretical Γ_R curve: $\omega_K\Gamma_A = (1 - \omega_K)\Gamma_R$.

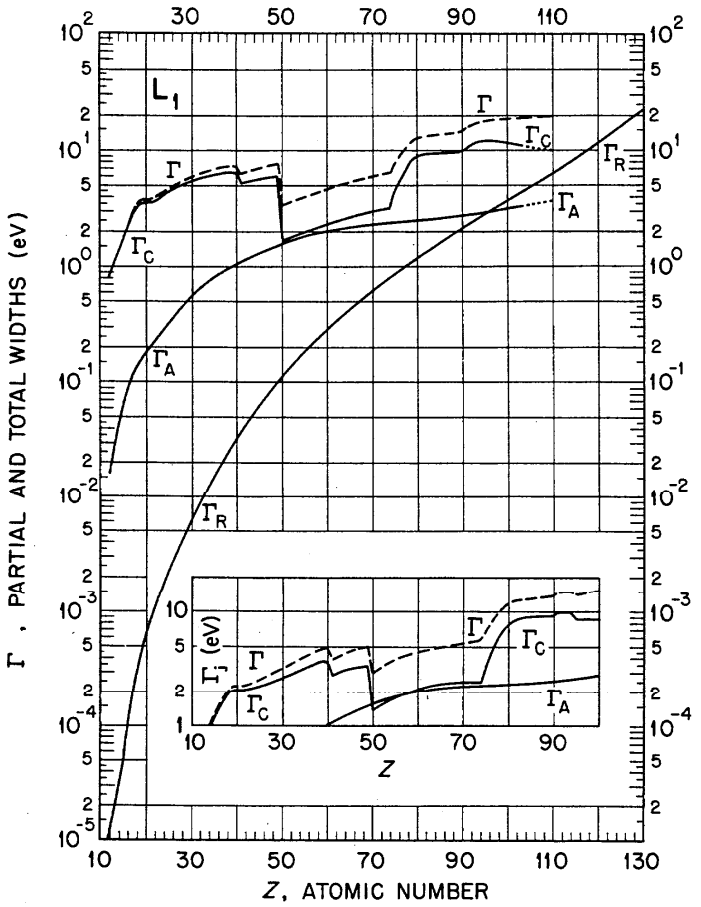

FIGURE 2. Theoretical partial and total atomic level widths for L_1 subshell. Γ_A = Auger width, Γ_C = Coster-Kronig width, Γ_R = radiative width, Γ = total width. Inset shows semi-empirical widths.

remaining regions, in which modifications are small, semi-empirical curves are not distinguished from theoretical curves in the graphic representation of figures 1 to 4.

Since calculations of Auger rates have not yet reached the same reliability as calculations of radiative rates, it is interesting in the case of the K shell to compare the theoretical Auger rate [14] with the semi-empirical Auger rate derived from the theoretical radiative rate [16–18] and the accurate, fitted fluorescence yield values (sec. 5.3). The result is shown in figure 1 and indicates that in the middle-to-high Z range the semi-empirical width (dot-dash curve) rises more slowly than the averaged theoretical prediction of Γ_A (solid curve). Assuming that this finding could be transferred to the L shell (generalization (2) in sec. 5.1.), the Auger widths Γ_A of the L subshells were modified analogously. The Γ_A curves in the insets of figures 2 and 3 incorporate this adjustment and show that a minor downward correction had to be applied at high Z.

5. Evaluation Procedure

In this work, all pertinent data were included in the evaluation process and judiciously weighed to obtain compatibility among the data of the different, but related properties (eqs (2) to (8), (11) and (12)). To achieve consistency between corresponding yields of individual subshells, strong reliance was placed on the *trends* of total and partial level widths plotted in figures 1 to 4. Stated and presumed accuracies were taken into account, but a least-squares adjustment for *all* data sets followed by a χ^2 test for consistency [19] could not be justified because of the use of theoretical predictions and the scarcity of experimental data in certain Z ranges. If in a given Z range input data of different types could not be mutually reconciled within their error limits, a judgement was made as to which set or sets of data were the most reliable.

The evaluation procedure adopted is outlined in the following sections, both in general terms and in detail.

5.1. Generalizations

The following generalizations were made for K and L shells:

(1) Partial and total level widths increase smoothly with atomic number Z, except at cutoffs and onsets of Coster-Kronig transitions (see figs. 1 to 4).

(2) Radiative and Auger widths of the different levels

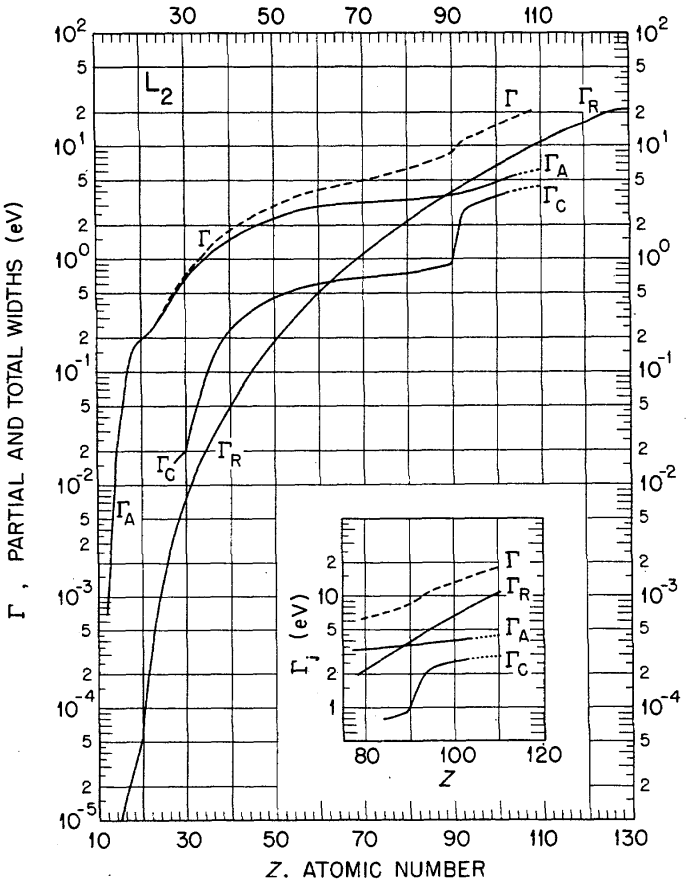

FIGURE 3. Theoretical partial and total atomic level width for L_2 subshell. Γ_A = Auger width, Γ_C = Coster-Kronig width, Γ_R = radiative width, Γ = total width. Inset shows semi-empirical widths.

display similar trends as a function of Z. As a consequence, fluorescence yields ω_K, ω_3, and ω_2 where Γ_C is small, will vary similarly (compare figs. 1 to 4). This characteristic has been used previously [3] to derive an analytical expression for ω_3 similar to that for ω_K.

(3) Relativistic Hartree-Fock values of the radiative widths [16,17] are considered reliable because of their agreement (a) with measured $K\alpha$ line widths [10,11] of the heavy elements in which the radiative component predominates, and in particular (b) with intensity ratios of x-ray emission lines [20] with final states in different principal shells, such as $K\beta$ and $K\alpha$ lines.

(4) Theory overestimates Coster-Kronig rates Γ_C.

5.2. Outline of Procedure

The evaluation procedure for the L subshells involved seven steps (for K shell see sec 5.3):

(1) Weighted least-squares fits to experimental yield data were made in regions where number and quality of measurements justified the procedure.

(2) Theoretical level widths Γ were modified in accordance with experimental data on level widths, x-ray line widths and Auger line widths (line widths corrected for width of other level(s) involved in transition). Partial widths Γ_C and sometimes Γ_A were modified correspondingly; in several instances, further information on Γ_C was derived from x-ray spectral data. Only those data on level and line widths were utilized for which absence of non-lifetime broadening [21,22] and reliability of measurements could be presumed. Partial and total level widths were extrapolated to $Z = 110$.

(3) Radiative and radiationless yields were calculated from modified theoretical rates of step (2).

(4) Semi-empirical values from step (3) were compared with experimental yield values, including fitted values from step (1), and the two sets of data were averaged according to the stated or presumed accuracies of all entries. In regions in which few or no measurements have been reported, results from step (3) were weighted more heavily than values obtained by extrapolation of the least-squares fits of step (1).

(5) Results from step (4) were smoothed, separately for each yield, as a function of Z.

(6) Values obtained in step (5) were checked against experimental fluorescence and Coster-Kronig yields and the semi-empirical results from step (3). This was done to assure that the averaging and smoothing steps did not introduce unacceptable slopes and fluctuations in the curves of partial widths (see points (1) and (2) of

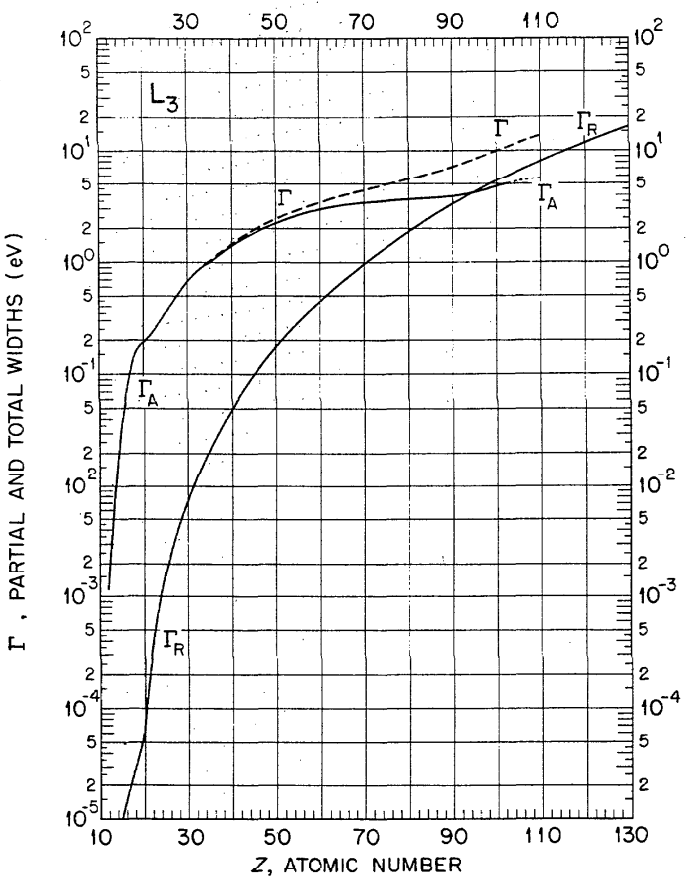

FIGURE 4. Theoretical partial and total atomic level widths for L_3 subshell. Γ_A = Auger width, Γ_R = radiative width, Γ = total width.

generalizations) or excessive deviations from the experimental data. Corrections were made if a need was indicated.

(7) Level widths Γ_i were calculated from the fluorescence yields of step (6) and theoretical radiative transition rates [16–18]. This step was done to assure that (a) the resulting width values of each subshell increased smoothly with Z, except at Coster-Kronig breaks, (point (1) of generalizations), and (b) combinations of Γ_i values were in reasonable agreement with experimental or evaluated widths of $KL_3\alpha_1$ and $KL_2\alpha_2$ x rays and the width difference of the $L_2M_4\beta_1$ and $L_3M_4\alpha_2$ x-ray lines [10,11]. A final smoothing adjustment was made in the fluorescence yield values and the complementary radiationless yields.

5.3. Details Concerning Individual Selections

The more important details in the evaluation are described in the following:

K Shell.

In the range $10 \leq Z \leq 93$, adopted values of ω_K represent the mean, weighted toward recent data (Appendix), between the selections by Bambynek et al. [2] and by Burhop and Asaad [3]. New data listed in the Appendix were utilized for $93 \leq Z \leq 99$. At low Z, only gas-target determinations were considered, and the datum for neon served as an anchor point. Solid-target data furnished the values given in table 1.

L_3 Subshell.

In the range $55 \leq Z \leq 96$, a least-squares fit was applied to the data compiled in references 2 and 3 and the Appendix. Results were averaged with those from the L_3 graph (fig. 4) on partial and total widths, whereby the width of the $L_3M_5\alpha_1$ line was taken into account [10]. Below $Z \simeq 55$, I emphasized the results taken from figure 4 and modified these in accordance with level widths determinations at $Z = 18$ and 30. Note that Γ_A was not allowed to increase as steeply near $Z = 95$ as shown in figure 4.

L_2 Subshell

In the range $60 \leq Z \leq 90$, least-squares-fit values of experimental ω_2 data were retained nearly unaltered, since they agree well with those obtained from the L_2 graph (fig. 3). Experimental $f_{2,3}$ values, especially those of recent origin, were found to agree satisfactorily with

the theoretical values obtained from figure 3. The latter values were adopted. On the basis of this accord the partial widths in figure 3 were trusted to supply reliable ω_2 and $f_{2,3}$ values also for $30 \leq Z \leq 60$. Values below $Z \approx 30$ were obtained from the theoretical partial widths (fig. 3) that were modified in accordance with the experimental widths data at $Z = 18$ and 30 for free atoms. Note that the transition L_2–$L_3 3d$ is forbidden in free atoms for $Z \leq 30$ [6,12] (as for $Z > 30$), but is allowed in metals for $26 \leq Z \leq 30$ and possibly to $Z = 22$ [23,24]. Estimates of yields for these metals are given in table 1. Adopted values for ω_2 and $f_{2,3}$ following the onset of L_2–L_3M_5 transitions at $Z = 91$ were derived from a compromise between the measured values and those from the inset of figure 3. I may point out that reducing Γ_C to about 2.5 eV yields satisfactory agreement with (a) the reported width differences [10] $\Gamma(L_2M_4\beta_1) - \Gamma(L_3M_4\alpha_2)$, (b) the general tendency of the calculations to overestimate Coster-Kronig rates, and (c) the average of all ω_2 values reported.

L_1 Subshell

Since the Coster-Kronig rate is the dominant component of the L_1 decay rate, its proper assessment will determine the quality of yield values in regions in which directly measured values are nonexistent or inaccurate. Preselected partial widths plotted in the inset of figure 2 were used to derive, with minor adjustments, the adopted ω_1 and f_1 values. Possible discontinuities were placed at $Z = 40,41$, $Z = 49,50$, $Z = 74,75$, $Z = 90,91$, and $Z = 104$ in accordance with cutoffs and onsets of Coster-Kronig transitions [12,25], but were ignored between $Z \approx 22$ and $Z \approx 35$ because of lack of precise information on the size of the jumps. The choices made for Γ_C and Γ_A at $Z \gtrsim 76$ gave ω_1 values that agree satisfactorily with experimental data, but f_1 values that are 10–15% lower than the majority of the measured values. Partitioning of f_1 into its $f_{1,2}$ and $f_{1,3}$ components followed the pattern suggested by theory. Intrashell radiative yield values, $f'_{1,3}$, were taken exclusively from Scofield's calculation [16,18], since virtually no experimental data are available. However, the only experiment [26] carried out so far, points to lower values than those calculated.

6. Estimate of Uncertainties

Presumed and stated reliability of input material, number or lack of measurements, and the degree of compatibility of the different relevant data determined the uncertainties assigned to the adopted values. Uncertainties in the various Z ranges are given in table 2.

7. Presentation of Output Data

The values of atomic fluorescence and Coster-Kronig yields that are tabulated in table 3 and plotted in figures 4 to 8 are the values adopted in section 5.2, step (7) of the evaluation procedure. Note that in this work the intrashell radiative yield $f'_{1,3}$ is contained in the L_1 subshell fluorescence yield ω_1. The same applies to the $f'_{1,2}$ component of the L_1 intrashell radiative yield; however since $f'_{1,2} << f'_{1,3}$ [16,18], the yield $f'_{1,2}$ is not listed separately in table 3.

The adopted values of the Auger yields are presented in table 4 and figures 5 to 8; these values were calculated from eq (8) using the values of fluorescence and Coster-Kronig yields of table 3.

The effective fluorescence yields for ionization in the L_1 and L_2 subshells are given in table 5 and figures 9 and 10; these values were obtained from eqs (9) and (10) using the entries of table 3. The corresponding yield ν_3 for the L_3 subshell is identical with ω_3; and it can be seen from tables 3 and 5 that the effective fluorescence yields for the three L subshells differ by less than 10% over most of the periodic table. Level widths were obtained as a set of output data in step (7) of the evaluation procedure (sec 5.2). The values that were calculated with the final, adopted values of the fluorescence yields are reported and discussed in the following paper [27].

As pointed out in sections 5.3 and 8, radiative and radiationless yields depend on the chemical structure in the light elements, in which transitions involve electrons which participate in bonding. However, little is known about the exact dependence of the yields, or transition rates, on the chemical structure for these light elements. It is with this *caveat* that the values for condensed matter listed in table 1 should be used.

Values of ω_K presented in table 1 were obtained from a curve fitted to experimental data ([2,3] and Appendix) for the metals Li, Be, B and Al, and the elemental solids C, P and S. Values of ω_2 and $f_{2,3}$ in table 1 were derived from the atomic radiative and Auger widths obtained in section 5 and experimental data [21,23] pertaining to the Coster-Kronig yield $f_{2,3}$ in the metals Zn and Cu. Theoretical Coster-Kronig rates [15], which were matched at $Z = 29$ to the experimental value, were used for $25 < Z < 29$ and extrapolated to $Z = 22$. No estimates of the yields for any of the L subshells are entered in table 1 for $Z \leq 21$, since virtually no experimental data are available for bound atoms in this range. However, it might be assumed, in analogy to the findings for the K shell, that the fluorescence yields would be smaller for the bound atoms than for the free atoms (table 3).

8. Problem Areas

In general, reduction of the data to single-hole atomic values has remained outside the capabilities of experiment and theory. This is of some concern in determining Coster-Kronig yields and assessing the reliability of the measured values. Investigations on the effect of double vacancies have not yet produced precise guidelines [28]; however, detailed results have become available of the effects of multiple vacancies on the fluorescence yields in several light atoms [29].

Table 1. Fluorescence, Auger and Coster-Kronig yields for light atoms in condensed matter.[a] (9.0 E-5 ≡ 9.0 × 10^{-5}).

K Shell			L_2 Subshell			
Z	ω_K	a_K	Z	ω_2	a_2	$f_{2,3}$
3	9.0 E-5	1.000	22	1.1 E-3[b]	0.75[b]	0.25[b]
4	3.3 E-4	1.000	23	1.8 E-3[b]	0.71[b]	0.29[b]
5	7.0 E-4	1.000	24	2.3 E-3[b]	0.65[b]	0.35[b]
6	1.4 E-3	0.999	25	3.1 E-3[b]	0.61[b]	0.39[b]
7	3.1 E-3	0.997	26	3.6 E-3	0.58	0.42
8	5.8 E-3	0.994	27	4.4 E-3	0.57	0.43
9	9.2 E-3	0.991	28	5.1 E-3	0.54	0.45
10	0.016	0.984	29	5.7 E-3	0.52	0.47
11	0.021	0.979	30	9.5 E-3	0.75	0.24
12	0.028	0.972				
13	0.036	0.964				
14	0.048	0.952				
15	0.061	0.939				

[a]K-shell values are based primarily on experimental determinations of ω_K (see Appendix). L_2-shell values take into account the rates of L_2–$L_3M_{4,5}$ Coster-Kronig transitions, which are energetically favored in the indicated range.
[b]Assuming the transition $2p_{1/2}$–$2p_{3/2}3d$ is allowed also for Z = 22 to 25.

In the range $88 \lesssim Z \lesssim 96$, several measured values of both ω_2 and $f_{2,3}$ lie above the adopted values for a given Z. Such data cannot be accommodated within the systematics of the rates detailed in figure 3, as this would require Γ_A to decrease sharply with increasing Z, or Γ_R to increase by 10 to 20%. Either alternative is difficult to accept. A similar situation pertains to the ω_1 and f_1 yields above $Z \approx 80$. Obviously, accurate measurements and careful considerations of double-hole effects are desirable in these regions.

Larger uncertainties occur for the K shell fluorescence yield below $Z = 10$ and the L shell fluorescence yield below $Z \approx 20$ since the adopted values were derived from data on molecules and from theoretical rates based on calculations in the single-particle model. However, in these regions transition rates may be altered substantially by many-body interactions [30] and chemical effects. The strong influence of many-body effects on Coster-Kronig transitions was recently demonstrated for the M shell [31]; these effects presumably occur also in the L shell, though probably to a lesser degree, and may result in a reduction of Γ_C similar to the semi-empirical reduction made in this work.

9. Acknowledgements

I am indebted to M. Schmorak for a computer search of literature, and especially to C. W. Nestor, Jr. for computer composition of the main tables and graphs. This work was sponsored by the U. S. Department of Energy, Division of Nuclear Sciences, Office of Basic Energy Sciences, under contract W- 7405- eng-26 with the Union Carbide Corporation, operator of the Oak Ridge National Laboratory.

Table 2. Estimated uncertainties (in percent) of adopted values for fluorescence and Coster-Kronig yields.

	Range of atomic numbers										
Yield	5–10	10–20	20–30	30–40	40–50	50–60	60–70	70–80	80–90	90–100	100–110
ω_K	40–10[a]	10–5	5–3	3	2	2–1	1	1	≲1	≲1	1
ω_1	–	≳30[a]	30[a]	30[b]	30–20[b]	20–15	15	15[b]	15	15–20	20
ω_2	–	≳25[a]	25[a,b]	25	25–10	10	10–5	5	5	10[b]	10
ω_3	–	≳25[a]	25[a]	20	20–10	10–5	5	5 3	3	3 5	5
f_1	–	3[a]	5[a]	5	5–10[b]	15	10	10–5[b]	5	5–10	15
$f_{1,2}$	–	10[a]	15[a]	15	20[b]	20	15	20[b]	10	10–50	50–100
$f_{1,3}$	–	5[a]	10[a]	10	10[b]	15	10	10–5[b]	5	5–10	15
$f_{2,3}$	–	–	≳40[a]	30–20	20	20	20–15	15	15	15[b]	20

[a]In these regions, yields for molecules and solids may differ from those for atoms by more than the values quoted.
[b]Near breaks in the yield curves, uncertainties may exceed those listed.

Table 3. Adopted values of fluorescence and Coster-Kronig yields[a]

Z		ω_K	ω_1	ω_2	ω_3	f_1	$f_{1,2}$	$f_{1,3}$	$f'_{1,3}$	$f_{2,3}$
5	B	1.7E-03								
6	C	2.8E-03								
7	N	5.2E-03								
8	O	8.3E-03								
9	F	0.013								
10	NE	0.018								
11	NA	0.023								
12	MG	0.030	2.9E-05	1.2E-03	1.2E-03	0.962	0.32	0.64	2.0E-05	
13	AL	0.039	2.6E-05	7.5E-04	7.5E-04	0.965	0.32	0.64	1.6E-05	
14	SI	0.050	3.0E-05	3.7E-04	3.8E-04	0.959	0.32	0.64	1.4E-05	
15	P	0.063	3.9E-05	3.1E-04	3.1E-04	0.951	0.32	0.63	1.2E-05	
16	S	0.078	7.4E-05	2.6E-04	2.6E-04	0.944	0.32	0.62	1.4E-05	
17	CL	0.097	1.2E-04	2.4E-04	2.4E-04	0.939	0.32	0.62	1.4E-05	
18	AR	0.118	1.8E-04	2.2E-04	2.2E-04	0.934	0.31	0.62	1.3E-05	
19	K	0.140	2.4E-04	2.7E-04	2.7E-04	0.929	0.31	0.62	1.2E-05	
20	CA	0.163	3.1E-04	3.3E-04	3.3E-04	0.920	0.31	0.61	1.4E-05	
21	SC	0.188	3.9E-04	8.4E-04	8.4E-04	0.912	0.31	0.60	1.4E-05	
22	TI	0.214	4.7E-04	1.5E-03	1.5E-03	0.902	0.31	0.59	1.5E-05	
23	V	0.243	5.8E-04	2.6E-03	2.6E-03	0.894	0.31	0.58	1.6E-05	
24	CR	0.275	7.1E-04	3.7E-03	3.7E-03	0.885	0.31	0.57	1.8E-05	
25	MN	0.308	8.4E-04	5.0E-03	5.0E-03	0.877	0.30	0.58	1.9E-05	
26	FE	0.340	1.0E-03	6.3E-03	6.3E-03	0.868	0.30	0.57	2.1E-05	
27	CO	0.373	1.2E-03	7.7E-03	7.7E-03	0.856	0.30	0.56	2.3E-05	
28	NI	0.406	1.4E-03	8.6E-03	9.3E-03	0.847	0.30	0.55	2.4E-05	0.028
29	CU	0.440	1.6E-03	0.010	0.011	0.839	0.30	0.54	2.6E-05	0.028
30	ZN	0.474	1.8E-03	0.011	0.012	0.831	0.29	0.54	2.8E-05	0.026
31	GA	0.507	2.1E-03	0.012	0.013	0.822	0.29	0.53	3.0E-05	0.032
32	GE	0.535	2.4E-03	0.013	0.015	0.815	0.28	0.53	3.2E-05	0.050
33	AS	0.562	2.8E-03	0.014	0.016	0.809	0.28	0.53	3.4E-05	0.063
34	SE	0.589	3.2E-03	0.016	0.018	0.804	0.28	0.52	3.6E-05	0.076
35	BR	0.618	3.6E-03	0.018	0.020	0.800	0.28	0.52	3.8E-05	0.088
36	KR	0.643	4.1E-03	0.020	0.022	0.797	0.27	0.52	4.1E-05	0.100
37	RB	0.667	4.6E-03	0.022	0.024	0.794	0.27	0.52	4.4E-05	0.109
38	SR	0.690	5.1E-03	0.024	0.026	0.790	0.27	0.52	4.7E-05	0.117
39	Y	0.710	5.9E-03	0.026	0.028	0.785	0.26	0.52	5.2E-05	0.126
40	ZR	0.730	6.8E-03	0.028	0.031	0.779	0.26	0.52	5.8E-05	0.132
41	NB	0.747	9.4E-03	0.031	0.034	0.713	0.10	0.61	7.8E-05	0.137
42	MO	0.765	0.010	0.034	0.037	0.712	0.10	0.61	8.1E-05	0.141
43	TC	0.780	0.011	0.037	0.040	0.711	0.10	0.61	8.8E-05	0.144
44	RU	0.794	0.012	0.040	0.043	0.709	0.10	0.61	9.6E-05	0.148
45	RH	0.808	0.013	0.043	0.046	0.705	0.10	0.60	1.0E-04	0.150
46	PD	0.820	0.014	0.047	0.049	0.700	0.10	0.60	1.1E-04	0.151
47	AG	0.831	0.016	0.051	0.052	0.694	0.10	0.59	1.2E-04	0.153
48	CD	0.843	0.018	0.056	0.056	0.688	0.10	0.59	1.4E-04	0.155
49	IN	0.853	0.020	0.061	0.060	0.681	0.10	0.59	1.6E-04	0.157
50	SN	0.862	0.037	0.065	0.064	0.439	0.17	0.27	3.0E-04	0.157
51	SB	0.870	0.039	0.069	0.069	0.448	0.17	0.28	3.2E-04	0.156
52	TE	0.877	0.041	0.074	0.074	0.455	0.18	0.28	3.4E-04	0.155
53	I	0.884	0.044	0.079	0.079	0.461	0.18	0.28	3.7E-04	0.154
54	XE	0.891	0.046	0.083	0.085	0.466	0.19	0.28	4.0E-04	0.154
55	CS	0.897	0.049	0.090	0.091	0.470	0.19	0.28	4.3E-04	0.154
56	BA	0.902	0.052	0.096	0.097	0.474	0.19	0.28	4.7E-04	0.153
57	LA	0.907	0.055	0.103	0.104	0.478	0.19	0.29	5.1E-04	0.153
58	CE	0.912	0.058	0.110	0.111	0.482	0.19	0.29	5.5E-04	0.153
59	PR	0.917	0.061	0.117	0.118	0.485	0.19	0.29	6.0E-04	0.153
60	ND	0.921	0.064	0.124	0.125	0.488	0.19	0.30	6.6E-04	0.152
61	PM	0.925	0.066	0.132	0.132	0.490	0.19	0.30	7.2E-04	0.151
62	SM	0.929	0.071	0.140	0.139	0.492	0.19	0.30	7.9E-04	0.150
63	EU	0.932	0.075	0.149	0.147	0.493	0.19	0.30	8.7E-04	0.149
64	GD	0.935	0.079	0.158	0.155	0.493	0.19	0.30	9.6E-04	0.147

Table 3. Adopted values of fluorescence and Coster-Kronig yields[a] – continued

Z		ω_K	ω_1	ω_2	ω_3	f_1	$f_{1,2}$	$f_{1,3}$	$f'_{1,3}$	$f_{2,3}$
65	TB	0.938	0.083	0.167	0.164	0.493	0.19	0.30	1.1E-03	0.145
66	DY	0.941	0.089	0.178	0.174	0.492	0.19	0.30	1.2E-03	0.143
67	HO	0.944	0.094	0.189	0.182	0.490	0.19	0.30	1.3E-03	0.142
68	ER	0.947	0.100	0.200	0.192	0.487	0.19	0.30	1.4E-03	0.140
69	TM	0.949	0.106	0.211	0.201	0.483	0.19	0.29	1.6E-03	0.139
70	YB	0.951	0.112	0.222	0.210	0.478	0.19	0.29	1.8E-03	0.138
71	LU	0.953	0.120	0.234	0.220	0.472	0.19	0.28	2.0E-03	0.136
72	HF	0.955	0.128	0.246	0.231	0.465	0.18	0.28	2.3E-03	0.135
73	TA	0.957	0.137	0.258	0.243	0.457	0.18	0.28	2.6E-03	0.134
74	W	0.958	0.147	0.270	0.255	0.447	0.17	0.28	2.8E-03	0.133
75	RE	0.959	0.144	0.283	0.268	0.485	0.16	0.33	3.0E-03	0.130
76	OS	0.961	0.130	0.295	0.281	0.552	0.16	0.39	2.9E-03	0.128
77	IR	0.962	0.120	0.308	0.294	0.603	0.15	0.45	2.8E-03	0.126
78	PT	0.963	0.114	0.321	0.306	0.640	0.14	0.50	2.8E-03	0.124
79	AU	0.964	0.107	0.334	0.320	0.672	0.14	0.53	2.8E-03	0.122
80	HG	0.965	0.107	0.347	0.333	0.690	0.13	0.56	3.0E-03	0.120
81	TL	0.966	0.107	0.360	0.347	0.696	0.13	0.57	3.2E-03	0.118
82	PB	0.967	0.112	0.373	0.360	0.696	0.12	0.58	3.5E-03	0.116
83	BI	0.968	0.117	0.387	0.373	0.694	0.11	0.58	3.8E-03	0.113
84	PO	0.968	0.122	0.401	0.386	0.689	0.11	0.58	4.2E-03	0.111
85	AT	0.969	0.128	0.415	0.399	0.685	0.10	0.59	4.7E-03	0.111
86	RN	0.969	0.134	0.429	0.411	0.682	0.10	0.58	5.2E-03	0.110
87	FR	0.970	0.139	0.443	0.424	0.677	0.10	0.58	5.8E-03	0.109
88	RA	0.970	0.146	0.456	0.437	0.672	0.09	0.58	6.4E-03	0.108
89	AC	0.971	0.153	0.468	0.450	0.664	0.09	0.58	7.1E-03	0.108
90	TH	0.971	0.161	0.479	0.463	0.660	0.09	0.57	7.8E-03	0.108
91	PA	0.972	0.162	0.472	0.476	0.664	0.08	0.58	8.4E-03	0.139
92	U	0.972	0.176	0.467	0.489	0.652	0.08	0.57	9.7E-03	0.167
93	NP	0.973	0.187	0.466	0.502	0.642	0.07	0.57	0.011	0.192
94	PU	0.973	0.205	0.464	0.514	0.605	0.05	0.56	0.013	0.198
95	AM	0.974	0.218	0.471	0.526	0.595	0.05	0.55	0.014	0.203
96	CM	0.974	0.228	0.479	0.539	0.587	0.04	0.55	0.016	0.200
97	BK	0.975	0.236	0.485	0.550	0.580	0.04	0.54	0.017	0.198
98	CF	0.975	0.244	0.490	0.560	0.573	0.03	0.54	0.019	0.197
99	ES	0.975	0.253	0.497	0.570	0.565	0.03	0.54	0.021	0.196
100	FM	0.976	0.263	0.506	0.579	0.556	0.03	0.53	0.023	0.194
101	MD	0.976	0.272	0.515	0.588	0.548	0.02	0.53	0.026	0.191
102	NO	0.976	0.280	0.524	0.596	0.540	0.02	0.52	0.028	0.189
103	LR	0.977	0.282	0.533	0.604	0.538	0.01	0.53	0.030	0.185
104		0.977	0.291	0.544	0.611	0.531	0.01	0.52	0.033	0.181
105		0.977	0.300	0.553	0.618	0.522	0.01	0.51	0.035	0.178
106		0.978	0.310	0.562	0.624	0.513		0.51	0.038	0.174
107		0.978	0.320	0.573	0.630	0.505		0.50	0.042	0.171
108		0.978	0.331	0.584	0.635	0.497		0.50	0.046	0.165
109		0.978	0.343	0.590	0.640	0.488		0.49	0.050	0.163
110		0.979	0.354	0.598	0.644	0.477		0.48	0.054	0.158

[a]Note: 1.7E–03 ≡ 1.7×10^{-3}; designation for L shell is omitted, read for example $\omega_1 = \omega_{L_1}$; $f_1 = f_{1,2} + f_{1,3}$; uncertainties are given in table 2.

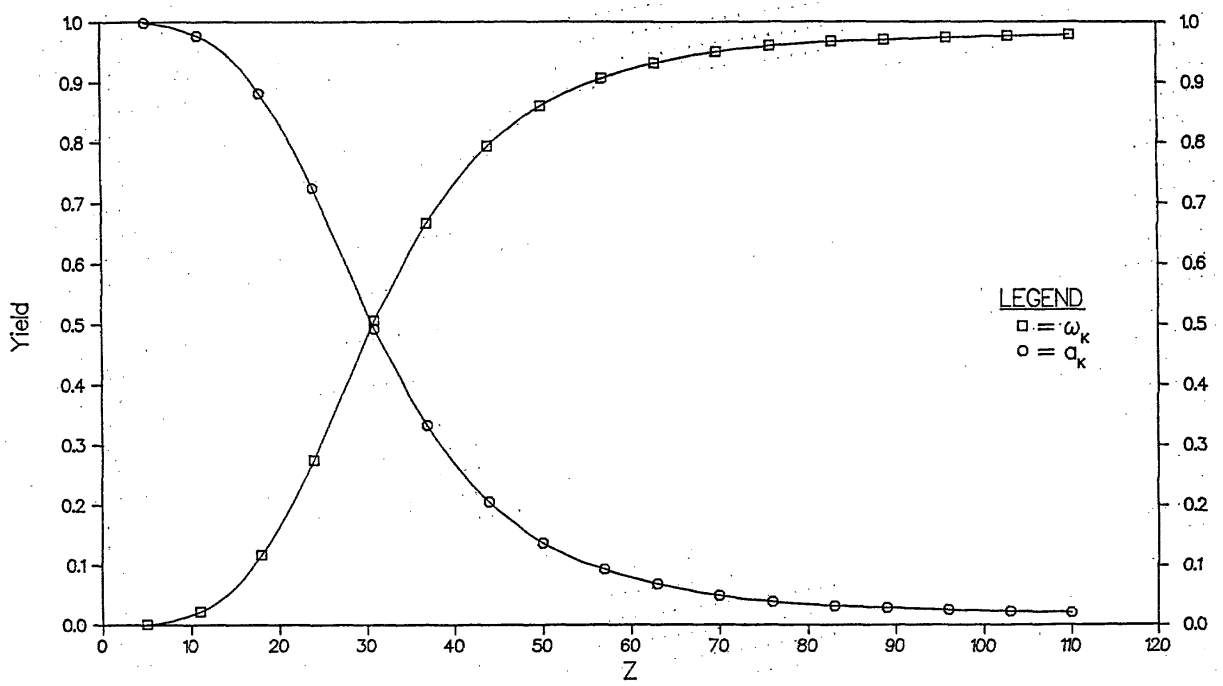

FIGURE 5. K shell fluorescence and Auger yields.

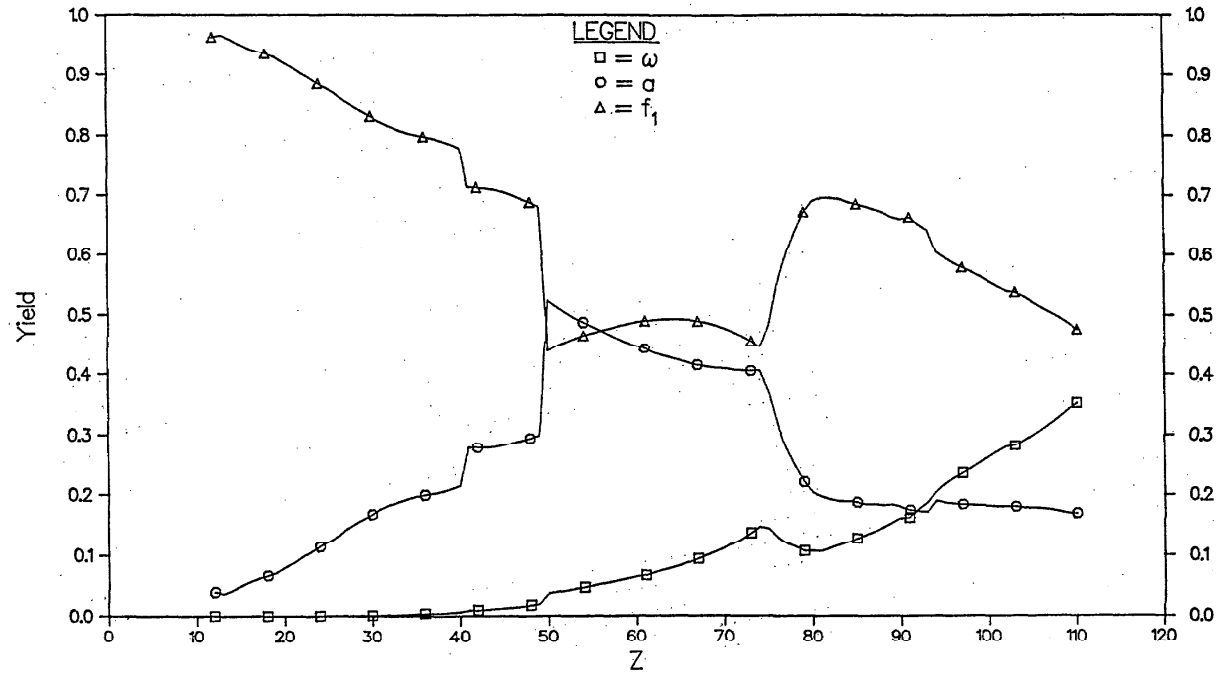

FIGURE 6. L_1 subshell fluorescence, Auger, and Coster-Kronig yields.

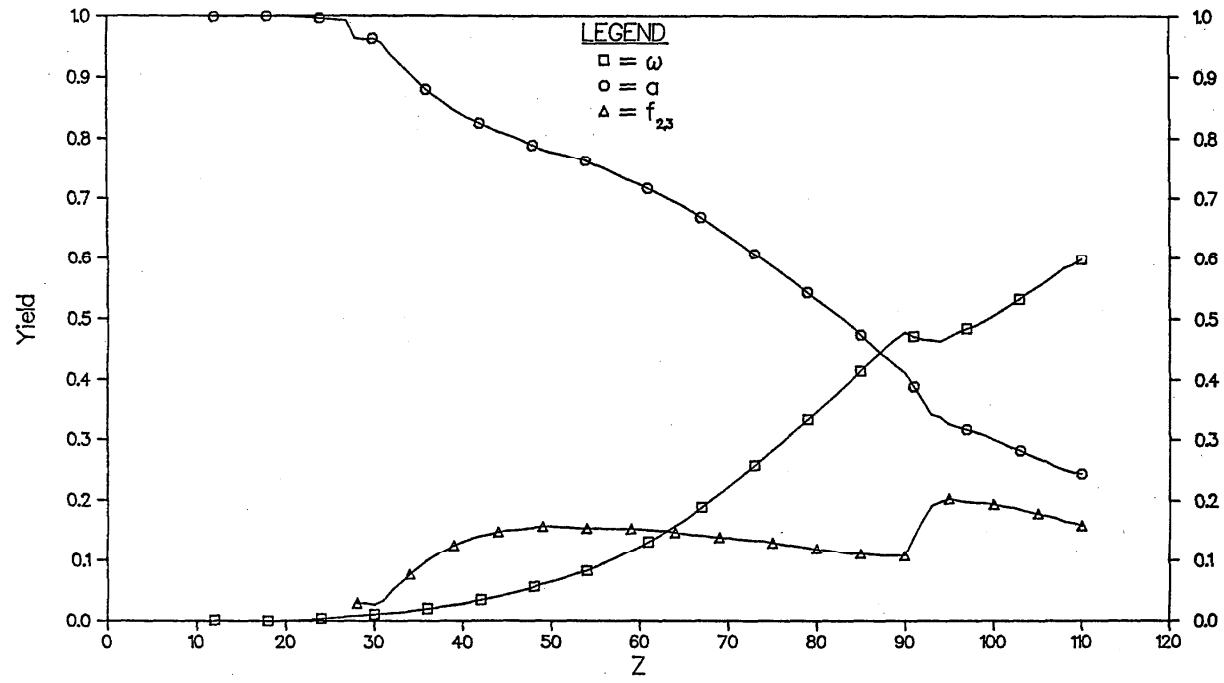

FIGURE 7. L_2 subshell fluorescence, Auger, and Coster-Kronig yields.

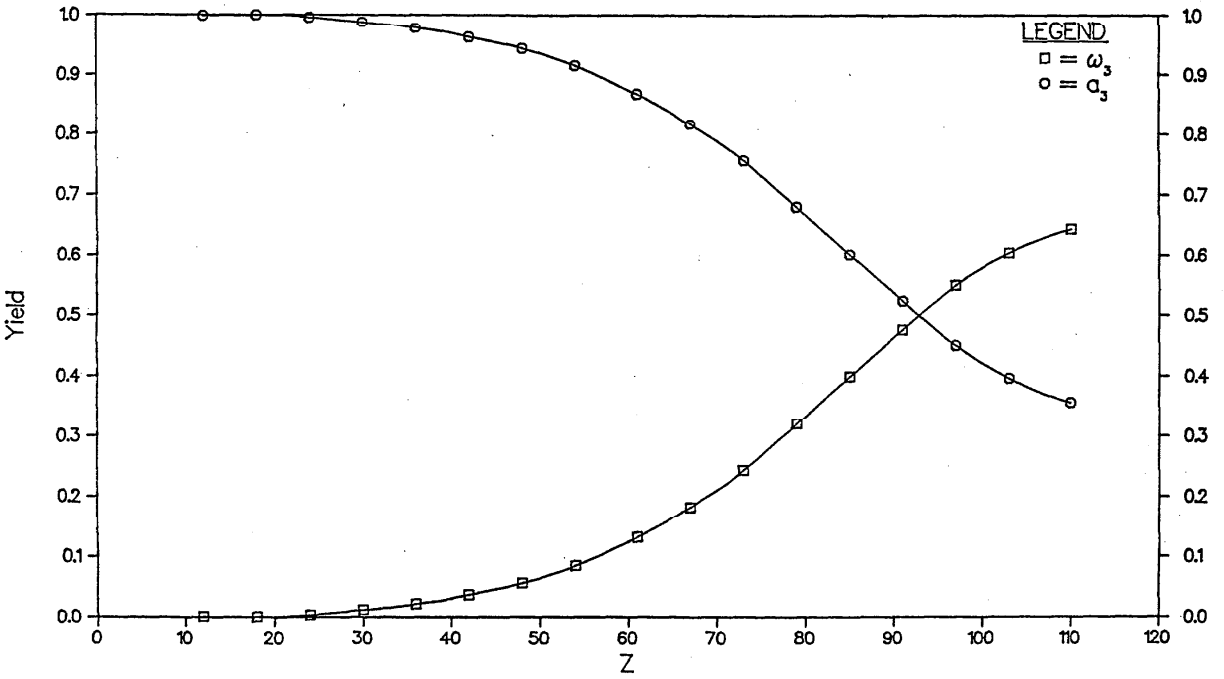

FIGURE 8. L_3 subshell fluorescence and Auger yields.

Table 4. Auger yields; values calculated from eq(8) with entries from table 3[a]

Z		a_K	a_1	a_2	a_3	Z		a_K	a_1	a_2	a_3
5	B	0.998				60	ND	0.079	0.448	0.724	0.875
6	C	0.997				61	PM	0.075	0.444	0.717	0.868
7	N	0.995				62	SM	0.071	0.437	0.710	0.861
8	O	0.992				63	EU	0.068	0.432	0.702	0.853
9	F	0.987				64	GD	0.065	0.428	0.695	0.845
10	NE	0.982				65	TB	0.062	0.424	0.688	0.836
11	NA	0.977				66	DY	0.059	0.419	0.679	0.826
12	MG	0.970	0.038	0.999	0.999	67	HO	0.056	0.416	0.669	0.818
13	AL	0.961	0.035	0.999	0.999	68	ER	0.053	0.413	0.660	0.808
14	SI	0.950	0.041	1.000	1.000	69	TM	0.051	0.411	0.650	0.799
15	P	0.937	0.049	1.000	1.000	70	YB	0.049	0.410	0.640	0.790
16	S	0.922	0.056	1.000	1.000	71	LU	0.047	0.408	0.630	0.780
17	CL	0.903	0.061	1.000	1.000	72	HF	0.045	0.407	0.619	0.769
18	AR	0.882	0.066	1.000	1.000	73	TA	0.043	0.406	0.608	0.757
19	K	0.860	0.071	1.000	1.000	74	W	0.042	0.406	0.597	0.745
20	CA	0.837	0.080	1.000	1.000	75	RE	0.041	0.371	0.587	0.732
21	SC	0.812	0.088	0.999	0.999	76	OS	0.039	0.318	0.577	0.719
22	TI	0.786	0.098	0.999	0.999	77	IR	0.038	0.277	0.566	0.706
23	V	0.757	0.105	0.997	0.997	78	PT	0.037	0.246	0.555	0.694
24	CR	0.725	0.114	0.996	0.996	79	AU	0.036	0.221	0.544	0.680
25	MN	0.692	0.122	0.995	0.995	80	HG	0.035	0.203	0.533	0.667
26	FE	0.660	0.131	0.994	0.994	81	TL	0.034	0.197	0.522	0.653
27	CO	0.627	0.143	0.992	0.992	82	PB	0.033	0.192	0.511	0.640
28	NI	0.594	0.152	0.963	0.991	83	BI	0.032	0.189	0.500	0.627
29	CU	0.560	0.159	0.962	0.989	84	PO	0.032	0.189	0.488	0.614
30	ZN	0.526	0.167	0.963	0.988	85	AT	0.031	0.187	0.474	0.601
31	GA	0.493	0.176	0.956	0.987	86	RN	0.031	0.184	0.461	0.589
32	GE	0.465	0.183	0.937	0.985	87	FR	0.030	0.184	0.448	0.576
33	AS	0.438	0.188	0.923	0.984	88	RA	0.030	0.182	0.436	0.563
34	SE	0.411	0.193	0.908	0.982	89	AC	0.029	0.183	0.424	0.550
35	BR	0.382	0.196	0.894	0.980	90	TH	0.029	0.179	0.413	0.537
36	KR	0.357	0.199	0.880	0.978	91	PA	0.028	0.174	0.389	0.524
37	RB	0.333	0.201	0.869	0.976	92	U	0.028	0.172	0.366	0.511
38	SR	0.310	0.205	0.859	0.974	93	NP	0.027	0.171	0.342	0.498
39	Y	0.290	0.209	0.848	0.972	94	PU	0.027	0.190	0.338	0.486
40	ZR	0.270	0.214	0.840	0.969	95	AM	0.026	0.187	0.326	0.474
41	NB	0.253	0.278	0.832	0.966	96	CM	0.026	0.185	0.321	0.461
42	MO	0.235	0.278	0.825	0.963	97	BK	0.025	0.184	0.317	0.450
43	TC	0.220	0.278	0.819	0.960	98	CF	0.025	0.183	0.313	0.440
44	RU	0.206	0.279	0.812	0.957	99	ES	0.025	0.182	0.307	0.430
45	RH	0.192	0.282	0.807	0.954	100	FM	0.024	0.181	0.300	0.421
46	PD	0.180	0.286	0.802	0.951	101	MD	0.024	0.180	0.294	0.412
47	AG	0.169	0.290	0.796	0.948	102	NO	0.024	0.180	0.287	0.404
48	CD	0.157	0.294	0.789	0.944	103	LR	0.023	0.180	0.282	0.396
49	IN	0.147	0.299	0.782	0.940	104		0.023	0.178	0.275	0.389
50	SN	0.138	0.524	0.778	0.936	105		0.023	0.178	0.269	0.382
51	SB	0.130	0.513	0.775	0.931	106		0.022	0.177	0.264	0.376
52	TE	0.123	0.504	0.771	0.926	107		0.022	0.175	0.256	0.370
53	I	0.116	0.495	0.767	0.921	108		0.022	0.172	0.251	0.365
54	XE	0.109	0.488	0.763	0.915	109		0.022	0.169	0.247	0.360
55	CS	0.103	0.481	0.756	0.909	110		0.021	0.169	0.244	0.356
56	BA	0.098	0.474	0.751	0.903						
57	LA	0.093	0.467	0.744	0.896						
58	CE	0.088	0.460	0.737	0.889						
59	PR	0.083	0.454	0.730	0.882						

[a]Designation for L shell is omitted, read for example $a_1 \equiv a_{L_1}$.

Table 5. Effective fluorescence yields for the L_1 and L_2 subshells; values calculated from eqs (9) and (10) with entries from table 3[a]

Z		ν_1	ν_2	Z		ν_1	ν_2	Z		ν_1	ν_2
10	NE			50	SN	0.067	0.075	90	TH	0.476	0.529
11	NA			51	SB	0.072	0.080	91	PA	0.485	0.538
12	MG	1.2E-03	1.2E-03	52	TE	0.077	0.085	92	U	0.503	0.549
13	AL	7.5E-04	7.5E-04	53	I	0.083	0.091	93	NP	0.518	0.562
14	SI	3.9E-04	3.7E-04	54	XE	0.088	0.096	94	PU	0.528	0.566
15	P	3.3E-04	3.1E-04	55	CS	0.094	0.104	95	AM	0.544	0.578
16	S	3.2E-04	2.6E-04	56	BA	0.100	0.111	96	CM	0.557	0.587
17	CL	3.5E-04	2.4E-04	57	LA	0.108	0.119	97	BK	0.566	0.594
18	AR	3.8E-04	2.2E-04	58	CE	0.114	0.127	98	CF	0.575	0.600
19	K	4.9E-04	2.7E-04	59	PR	0.121	0.135	99	ES	0.591	0.609
20	CA	6.1E-04	3.3E-04	60	ND	0.129	0.143	100	FM	0.602	0.618
21	SC	1.2E-03	8.4E-04	61	PM	0.135	0.152	101	MD	0.611	0.627
22	TI	1.8E-03	1.5E-03	62	SM	0.143	0.161	102	NO	0.619	0.637
23	V	2.9E-03	2.6E-03	63	EU	0.152	0.171	103	LR	0.627	0.645
24	CR	4.0E-03	3.7E-03	64	GD	0.160	0.181	104		0.635	0.655
25	MN	5.2E-03	5.0E-03	65	TB	0.169	0.191	105		0.643	0.663
26	FE	6.5E-03	6.3E-03	66	DY	0.180	0.203	106		0.652	0.671
27	CO	7.8E-03	7.7E-03	67	HO	0.190	0.215	107		0.661	0.681
28	NI	9.2E-03	8.9E-03	68	ER	0.201	0.227	108		0.678	0.689
29	CU	0.011	0.010	69	TM	0.210	0.239	109		0.689	0.694
30	ZN	0.012	0.011	70	YB	0.221	0.251	110		0.698	0.700
31	GA	0.013	0.012	71	LU	0.232	0.264				
32	GE	0.014	0.014	72	HF	0.243	0.277				
33	AS	0.015	0.015	73	TA	0.258	0.291				
34	SE	0.017	0.017	74	W	0.271	0.304				
35	BR	0.020	0.020	75	RE	0.284	0.318				
36	KR	0.022	0.022	76	OS	0.293	0.331				
37	RB	0.024	0.025	77	IR	0.305	0.345				
38	SR	0.026	0.027	78	PT	0.318	0.359				
39	Y	0.028	0.030	79	AU	0.330	0.373				
40	ZR	0.031	0.032	80	HG	0.345	0.387				
41	NB	0.034	0.036	81	TL	0.358	0.401				
42	MO	0.036	0.039	82	PB	0.372	0.415				
43	TC	0.040	0.043	83	BI	0.382	0.429				
44	RU	0.043	0.046	84	PO	0.396	0.444				
45	RH	0.046	0.050	85	AT	0.411	0.459				
46	PD	0.049	0.054	86	RN	0.422	0.474				
47	AG	0.053	0.059	87	FR	0.436	0.489				
48	CD	0.058	0.065	88	RA	0.448	0.503				
49	IN	0.062	0.070	89	AC	0.464	0.517				

[a]Note: 1.2E–03 ≡ 1.2×10^{-3}.

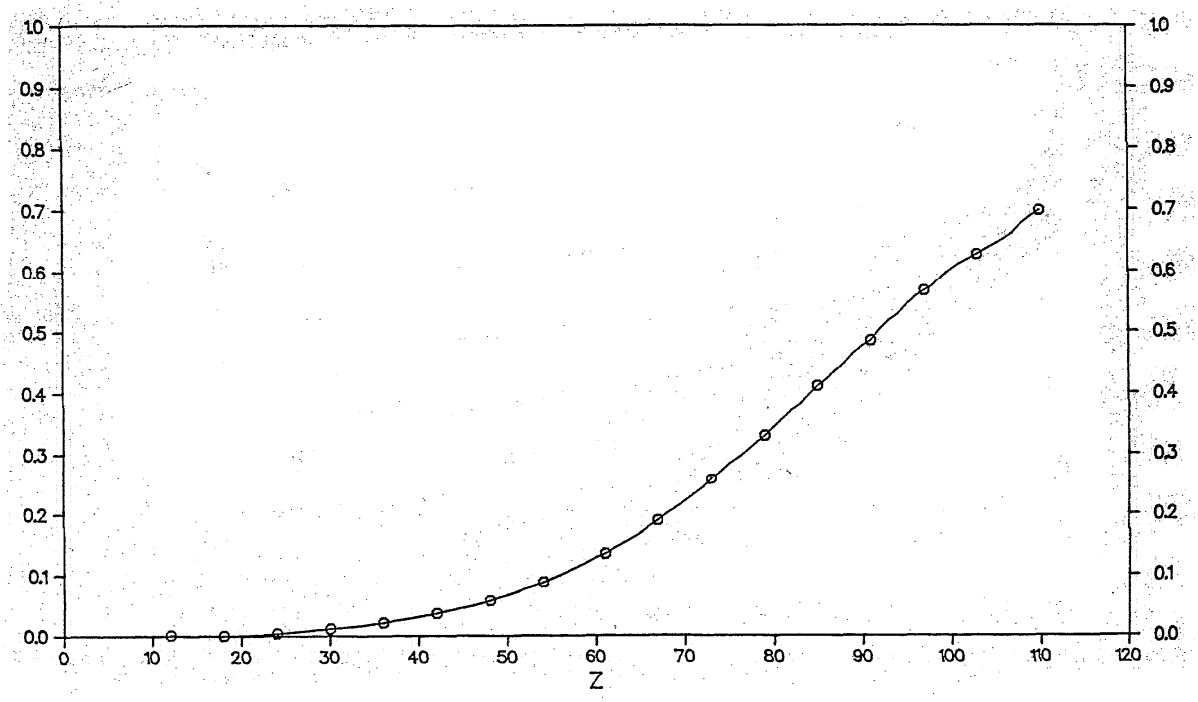

FIGURE 9. L_1 subshell effective fluorescence yield.

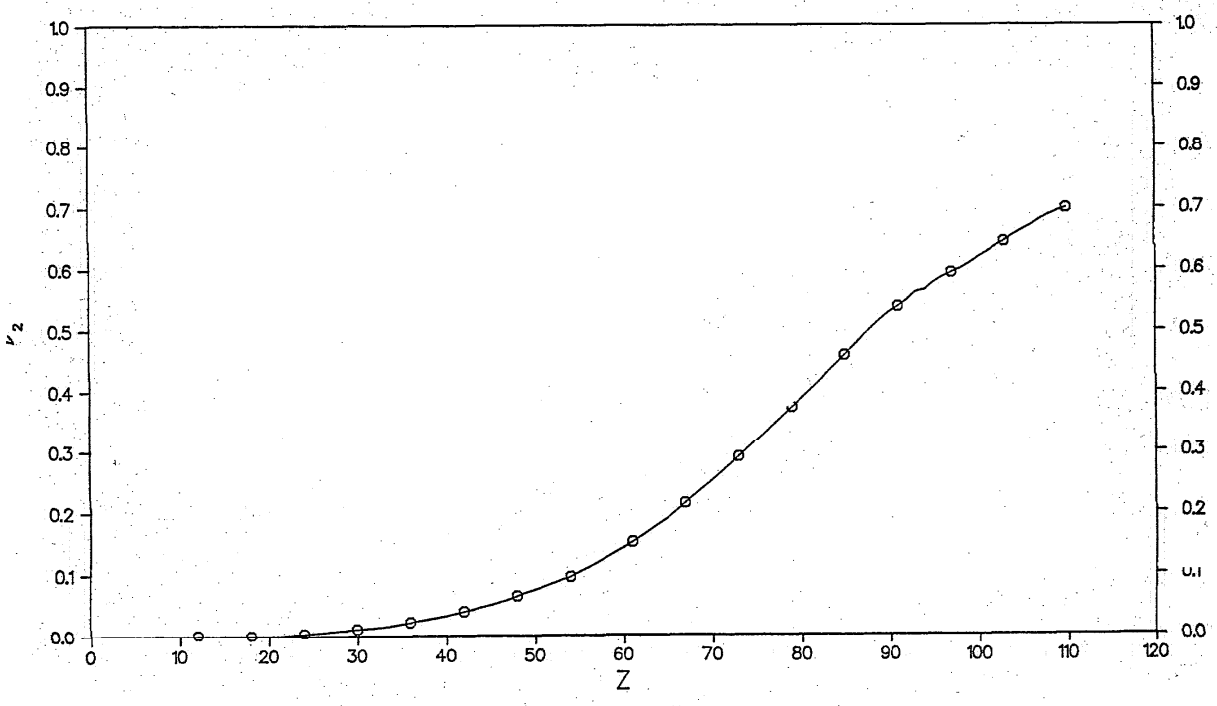

FIGURE 10. L_2 subshell effective fluorescence yield.

References

[1] Fink, R. W., Jopson, R. C., Mark, H., and Swift, C. D., Rev. Mod. Phys. **38**, 513 (1966).

[2] Bambynek, W., Crasemann, B., Fink, R. W., Freund, H-U., Mark, H., Swift, C. D., Price, R. E., and Rao, P. V., Rev. Mod. Phys. **44**, 716 (1972).

[3] Burhop, E. H. S., and Asaad, W. N., Adv. in Atomic and Molecular Physics, Vol. 8, 163 (1972).

[4] Listengarten, M. A., Izv. Akad. Nauk, SSSR, Ser. Fiz. 24, 1041 (1960). [Bull. Acad. Sci. USSR, Phys. **24**, 1050 (1960)].

[5] Fink, R. W., and Rao, P. V. in *Handbook of Spectroscopy*, J. W. Robinson, ed., pp. 219–229, CRC Press, Cleveland, Ohio (1974); *ibid.* (1978).

[6] Manson, S. T., Dehmer, J. L., and Inokuti, M., Bull. Am. Phys. Soc. **22**, 1332 (1977).

[7] Sevier, K. D., *Low Energy Electron Spectrometry, 397 pp., Wiley, Interscience, New York (1972).*

[8] *McGuire, E. J., "Auger and Coster-Kronig Transitions," in Atomic Inner-Shell Processes*, B. Crasemann, editor, Vol. 1, pp. 293–330, Academic Press, Inc., New York (1975).

[9] Parratt, L. G., Rev. Mod. Phys. **31**, 616 (1959).

[10] Salem, S. I., and Lee, P. L., At. Data Nucl. Data Tables, **18**, 233 (1976).

[11] Pessa, V. M., X-Ray Spectrometry, **2**, 169 (1973).

[12] Chen, M. H., Crasemann, B., Huang, K.-N., Aoyagi, M., and Mark, H., At. Data Nucl. Data Tables, **19**, 97 (1977).

[13] Keski-Rahkonen, O., and Krause, M. O., At. Data Nucl. Data Tables, **14**, 139 (1974).

[14] McGuire, E. J., Phys. Rev. A**2**, 273 (1970); Kostroun, V. O., Chen, M. H., and Crasemann, B., Phys. Rev. A**3**, 533 (1971); Bhalla, C. P., and Ramsdale, D. J., Z. Phys. **239**, 95 (1970); Bhalla, C. P., Rosner, H. R., and Ramsdale, D. J., J. Phys. B**3**, 1232 (1970).

[15] McGuire, E. J., Phys. Rev. A**3**, 1801 (1971); in *Inner Shell Ionization Phenomena and Future Applications*, Fink, R. W., Manson, S. T., Palms, J. M., Rao, P. V., editors, USAEC CONF–720404 (1973), pp. 662–679; Crasemann, B., Chen, M. H., and Kostroun, V. O., Phys. Rev. A**4**, 2161 (1971); Chen, M. H., Crasemann, B., and Kostroun, V. O., Phys. Rev. A**4**, 1 (1971); Yin, Lo I., Adler, I., Chen, M. H., and Crasemann, B., Phys. Rev. A**7**, 897 (1973); Walters, D. L. and Bhalla, C. P., Phys. Rev. A**4**, 2164 (1971).

[16] Scofield, J. H., Phys. Rev. A**9**, 1041 (1974); Phys. Rev. A**10**, 1507 (1974); and "Radiative Transitions" in *Atomic Innershell Processes*, B. Crasemann, editor, Vol. 1, pp. 265–288, Academic Press, Inc., New York (1975).

[17] Anholt, R., and Rasmussen, J. O., Phys. Rev. A**9**, 585 (1974).

[18] Scofield, J. H., At. Data Nucl. Data Tables **14**, 121 (1974).

[19] Bearden, J. A., and Thomsen, J. S., Nuovo Cimento **5**, 267 (1957).

[20] Salem, S. I., Panossian, S. L., and Krause, R. A., At. Data Nucl. Data Tables **14**, 91 (1974).

[21] Citrin, P. H., Eisenberger, P. M., Marra, W. C., Åberg, T., Utriainen, J., and Källne, E., Phys. Rev. B**10**, 1762 (1974).

[22] Kowalczyk, S. P., Ley, L., McFeely, F. R., and Shirley, D. A., Phys. Rev. B**11**, 1721 (1975).

[23] Matthew, J. A. D., Nuttall, J. D., and Gallon, T. E., J. Phys. C**9**, 883 (1976); Antonides, E., and Sawatzky, G. A., J. Phys. C**9**, L547 (1976); Yin, L. I., Adler, I., Chen, M. H., and Crasemann, B., Phys. Rev. A**7**, 897 (1973); Weightman, P., McGilp, J. F., and Johnson, C. E., J. Phys. C**9**, L585 (1976).

[24] Shirley, D. A., Martin, R. L., Kowalczyk, S. P., McFeely, F. R., and Ley, L., Phys. Rev. B**15**, 544 (1977).

[25] Doyle, B. L., and Shafroth, S. M. (private communication).

[26] Baker, K. R., Tolea, F., Fink, R. W., and Pinajian, J. J., Z. Physik **270**, 1 (1974).

[27] Krause, M. O., and Oliver, J. H., J. Phys. Chem. Ref. Data **8** 329 (1979).

[28] Campbell, J. L., McNelles, L. A., Geiger, J. S., Merritt, J. S., and Graham, R. L., Can. J. Phys. **55**, 868 (1977) and references therein.

[29] Kauffman, R. L., and Richard, P. in *Methods of Experimental Physics*, Academic Press, 1976, p. 148, and references therein.

[30] Kelly, H. P., in *Atomic Inner Shell Processes*, B. Crasemann, editor, Vol. I, p. 331, Adademic Press, Inc., New York (1975) and in *Photoionization and Other Probes of Many-Electron Interactions*, F. J. Wuilleumier, editor, Plenum Press, New York and London (1976), p. 83.

[31] Ohno, M. and Wendin, G., Physica Scripta **16**, 299 (1977).

APPENDIX. Reference list

Listing comprises work subsequent to the reviews by Bambynek, *et al.* (1972), Burhop and Assad (1972) and Sevier (1972). Cut-off date October 1977.

Z Element	Data reported	Notes Expt.: Experiment Th.: Theory	Reference
3 Li 6 C	ω_K = 1.06(53) E-4 ω_K = 1.3(4) E-3	Expt.; solid target	K. Feser, *Phys. Rev. Lett.* **29**, 901 (1972).
3 Li 11 Na	$\Gamma(K)$ = 0.02 eV $\Gamma(L_{2,3})$ = 0.02 eV	Th.; many-body; from Auger rate	A. J. Glick and A. L. Hagen, *Phys. Rev.* B15, 1950 (1977)
4 Be	ω_K = 2.15 E-5 ω_K – partial	Th.; many-body	H. P. Kelly, *Phys. Rev.* A9, 1582 (1974).
4 Be	ω_K – partial	Th.; many-body	F. Bely-Dubau, J. Dubau, and D. Petrini, *J. Phys.* B10, 1613 (1977)
4 Be 5 B	ω_K = 3.6(1.1) E-4 ω_K = 5.7(1.7) E-4	Expt.; solid target	K. Feser, *Phys. Rev. Lett.* **28**, 1013 (1972).
4 Be 5 B 6 C	ω_K = 3.0(6) E-4 ω_K = 7.1(2.8) E-4 ω_K = 1.13(22) E-3	Expt.; solid target	C. E. Dick and A. C. Lucas, *Phys. Rev.* A2, 580 (1970).
6 C	ω_K = 3.5(4) E-3	Expt.; solid target	W. Hink and H. Paschke, *Phys. Rev.* A4, 507 (1971)
6 C	ω_K = 2.46(35) E-3	Expt.; solid-gas combination	G. Bissinger, J. M. Joyce, and H. Kugel, *Phys. Rev.* A14, 1375 (1976).
6 C	ω_K = 2.2(2) E-3	Expt.; solid-gas combination	A. Langenberg and J. Van Eck, *Phys. Rev. Lett.* 31, 71 (1973)
6 C	ω_K = 1.5(7) E-3	Expt.; CH_4; gas target	L. H. Toburen, *Phys. Rev.* A5, 2482 (1972).
6 C 7 N 10 Ne	ω_K = 2.43(41) E-3 ω_K = 5.07(56) E-3 ω_K = 0.018(2)	Expt.; CH_4 N_2	A. Langenberg and J. Van Eck, *J. Phys.* B9, 2421 (1976).
6 C 7 N 10 Ne 18 Ar	ω_K = 2.69(39) E-3 ω_K = 4.73(68) E-3 ω_K = 0.0155(22) ω_K = 0.122(21)	Expt.; CH_4 N_2	H. Tawara, K. G. Harrison, and F. J. de Heer, *Physica* 63, 351 (1973)
10 Ne	Γ_A = 0.22 eV	Th; many-body	H. P. Kelly, *Phys. Rev.* A11, 556 (1975).
10 Ne	ω_K – partial	Th.	C. P. Bhalla, *Phys. Rev.* A12, 122 (1975).
10 Ne	ω_K = 0.016	Th.; variation of ω_K with hole configurations	C. P. Bhalla, N. O. Folland, and M. A. Hein, *Phys. Rev.* A8, 649 (1973); C. P. Bhalla, *J. Phys.* B8, 1200; 2787; 2792 (1975).
10 Ne	ω_K = 0.0159	Th.; Auger and radiative rates for KL^i hole configurations with i = 0 to 6.	M. H. Chen and B. Crasemann, *Phys. Rev.* A12, 959 (1975).
10 Ne	ω_K = 0.018	Expt.	N. Stolterfoht, D. Schneider, D. Burch, B. Aagard, E. Bøving, and B. Fastrup, *Phys. Rev.* A12, 1313 (1975).
10 Ne	ω_K = 0.017	Expt.; variation of ω_K with hole configuration	D. Schneider, Diss., Freie Univ. Berlin (1975); N. Stolterfoht, D. Schneider, and D. Burch, *Proc. IVth Int. Conf. on Atomic Physics*, Heidelberg (1974), p. 643.
10 Ne	$\Gamma(K)$ = 0.23(2) eV	Expt.; photoelectron	U. Gelius, *J. Electron Spectrosc.* 5, 1985 (1974).
10 Ne	$\Gamma(K)$ = 0.21(2) eV	Expt.; Auger	N. Stolterfoht, *4th Conf. Application of Small Accelerators.* Publ. Nr. 76CH117-9 NTS; Denton, Texas, Oct. 1976.
10 Ne	$\Gamma(K)$ = 0.27(5) eV	Expt.; x-ray lines	H. Ågren, J. Nordgren, L. Selander, C. Nordling, and K. Siegbahn, *Physica Scripta* (to be published, 1977/78).
11 Na	$\Gamma(K)$ = 0.27 eV $\Gamma(L_1)$ = 0.4 eV	Th.; Auger lines; free atom	H. Hillig, B. Cleff, W. Mehlhorn, and W. Schmitz, *Z. Physik* 268, 225 (1974).
12 Mg	$\Gamma(K)$ = 0.30(5) eV $\Gamma(L_1)$ = 0.7 eV	Expt.; Auger lines; free atom	B. Breuckmann and V. Schmidt, *Z. Physik* 268, 235 (1974).
13 Al	$\Gamma(K)$ = 0.36(5)	Expt.; x-ray lines; solid target	C. Senemaud, *Compt. Rend.* (Paris), B265, 403 (1971); Thesis, Univ. Paris VI (1969).
14 Si	$\Gamma(L_1)$ = 0.6(1) eV	Expt.; x-ray lines; solid target	E. Zöpf, *Phys. Lett.* 48A, 105 (1974).
15 P 16 S	ω_K = 0.056(3) ω_K = 0.077(4)	Expt.	A. Konstantinov and T. E. Sazonova, *Atlanta Conf. Proc.* (1973)*, p.158.
15 P 16 S	ω_K = 0.061(3) ω_K = 0.082(3)	Expt.	A. Molik, *Atlanta Conf. Proc.* (1973)*, p. 116.

APPENDIX. Reference list – continued

Listing comprises work subsequent to the reviews by Bambynek, *et al.* (1972), Burhop and Assad (1972) and Sevier (1972). Cut-off date October 1977.

Z Element	Data reported	Notes Expt.: Experiment Th.: Theory	Reference
17 Cl	ω_K = 0.095(4)		
	ω_K = 0.103(3)		
18 Ar	ω_K = 0.121(3)		
16 S	$\Gamma(K)$ = 0.6(1) eV	Expt.; H_2S, referred to Ar $\Gamma(K)$ = 0.67 eV	O. Keski-Rahkonen and M. O. Krause, *Phys. Rev.* A15, 959 (1977).
17 Cl	$\omega_{2,3}$ = 6.0(2.6) E-4	Expt.; HCl	Th. P. Hoogkamer, F. W. Saris and F. J. de Heer, *J. Phys.* B8, L105 (1975).
	$\omega_{2,3}$ = 4.9(2.4) E-4	Cl_2	
18 Ar	$\omega_{2,3}$ = 4.2(1.2) E-4		
18 Ar	$\omega_{2,3}$	Th.; variation with hole configuration	F. W. Saris and C. P. Bhalla, *J. Phys.* B7, L115 (1974).
18 Ar	$\omega_{2,3}$ = 2.3(9) E-4	Expt.; values of $\omega_{2,3}$ for different hole configurations	A. Langenberg, F. J. de Heer, and J. Van Eck, *J. Phys.* B8, 2079 (1975). N. Stolterfoht, F. J. de Heer, and J. Van Eck, *Phys. Rev. Lett.*, 30, 1159 (1973).
18 Ar	f_1 = 0.96(1)	Expt.; Auger and Coster-Kronig spectra	N. Stolterfoht, D. Schneider and P. Ziem, *Phys. Rev.* A10, 81 (1974).
18 Ar	ω_K = 0.130	Th.; variation with hole configuration	F. P. Larkins, *J. Phys.* B4, L29 (1971).
	$\omega_{2,3}$ = 1.9 E-4		
18 Ar	ω_K = 0.12	Expt.; 30 MeV Cl^{+6} projectiles	R. L. Cocke, R. R. Randall, S. L. Varghese, and B. Curnette, *Phys. Rev.* A14, 2026 (1976).
18 Ar	ω_K = 0.120	Th.; variation with hole configuration	C. P. Bhalla, *Phys. Rev.* A8, 2877 (1973).
18 Ar	$\omega_{2,3}$ = 1.48 E-4	Th.; variation with hole configuration	M. H. Chen and B. Crasemann, *Phys. Rev.* A10, 2232 (1974).
18 Ar	$\Gamma(K)$ = 0.77(10)	Expt.; Auger; assuming $\Gamma(L_2L_3)$ = 0.23 eV	M. O. Krause, *Phys. Rev. Lett.* 34, 633 (1975).
18 Ar	$\Gamma(K)$ = 0.69 eV	Expt.; Auger; assuming $\Gamma(L_2L_3)$ = 0.23 eV	L. Asplund, P. Kelfve, B. Blomster, H. Siegbahn and K. Siegbahn, *Physica Scripta* (to be published 1977/78).
18 Ar	$\Gamma(L_{2,3})$ = 0.12 eV	Expt.; x-ray lines	J. Nordgren, H. Ågren, C. Nordling and K. Siegbahn, *Physica Scripta* (to be published 1977/78).
	$\Gamma(L_1)$ = 1.3 eV		
18 Ar	$\Gamma(L_{2,3})$ = 0.10(2) eV	Expt.; Auger	D. Ridder, J. Dieringer and N. Stolterfoht, *J. Phys.* B9, L307 (1976).
18 Ar	$\Gamma(L_{2,3})$ = 0.10(2)	Expt.; Auger	T. Kondow, T. Kawai, K. Kunimori, T. Onishi, and K. Tamura, *J. Phys.* B6, L156 (1973).
23-32	$\Gamma(K\alpha_1)$ and $\Gamma(K\alpha_2)$	Expt.	P. L. Lee and S. I. Salem, *Phys. Rev.* A10, 2027 (1974).
	ω_2; ω_3	Semi-empirical	
24 Cr	ω_K = 0.267(4)	Expt.	A. A. Konstantinov, T. E. Sazonova, and A. Konstantinov, *Atlanta Conf. Proc.* (1973)*, p. 144.
24 Cr	ω_K = 0.284(10)	Expt.	A. Mukerii and L. Chin, *Atlanta Conf. Proc.* (1973)*. p. 164
25 Fe	ω_K = 0.358(18)		
30 Zn	ω_K = 0.442(11)		
25 Mn	ω_K = 0.322(5)	Expt.	Lj. Dobrilović, Dj. Bęk-Uzarov, M. Simović, K. Buraei, and A. Milojević, *Atlanta Conf. Proc.* (1973)*, p. 128.
26-94	ω_2; $f_{2,3}$	Th.	M. H. Chen and B. Crasemann, *Atlanta Conf. Proc.* (1973)*, p. 43.
27 Co	$L_{2,3}$ Auger spectra	Expt.; $L_3$3d3d/$L_2$3d3d intensity ratios in solids	J. A. D. Matthew, J. D. Nuttall, and T. E. Gallon, *J. Phys.* C9, 883 (1976).
28 Ni			
29 Cu			
30 Zn			
29 Cu	$\Gamma(L_2)$ = 0.98(4) eV	Expt.; Auger and photo-electron; solid target	Lo I. Yin, I. Adler, M. H. Chen and B. Crasemann, *Phys. Rev.* A7, 897 (1973).
	$\Gamma(L_3)$ = 0.54(3) eV		
30 Zn	$\Gamma(L_2)$ = 0.84(4) eV		
	$\Gamma(L_3)$ = 0.66(3) eV		
29-31	$\Gamma(L_{2,3})$; Γ_{CK}, ω_3	Th.; variation with Coster-Kronig transition cut-offs	
29-32	Γ (Auger lines)	Expt.; Coster-Kronig transition cut-offs; Auger satellites	E. Antonides, E. C. Janse, and G. A. Sawatzki, *Phys. Rev.* B15, 1669 and 4569 (1977).
	Γ (photolines)		
30 Zn	$\Gamma(L_2)$ = 0.47(5)eV	Expt.; photo-electron; solid target	P. Weightman, J. F. McGilp and C. E. Johnson, *J. Phys.* C9, L585 (1976).
	$\Gamma(L_3)$ = 0.33(5)eV		

APPENDIX. Reference list — continued

...isting comprises work subsequent to the reviews by Bambynek, *et al.* (1972), Burhop and Assad (1972) and Sevier (1972). Cut-off date October 1977.

Z Elemen.	Data reported	Notes Expt.: Experiment Th.: Theory	Referenc
30 Zn	$\Gamma(L_2) - \Gamma(L_3) = 0.19$ eV	Expt.; Auger spectra, solid metallic target	E. Antonides and G. A. Sawatzky, *J. Phys.* C9, L547 (1976).
	$\Gamma(L_2) - \Gamma(L_3) = 0.04$ eV	dto.; ZnO	
30 Zn	$\Gamma(L_2) = \Gamma(L_3)$	Expt.; photo-electron; solid target	L. Ley, S. P. Kowalczyk, F. R. McFeely, R. A. Pollak, and D. A. Shirley, *Phys. Rev.* B8, 2392 (1973).
30 Zn	$\Gamma(L_2) = \Gamma(L_3)$	Expt.; photo-electron; free atom	M. S. Banna, D. C. Frost, C. A. McDowell, and B. Wallbank, *J. Chem. Phys.* (1978).
30 Zn	$\Gamma(L_{2,3}) = 0.50(15)$ eV $\Gamma(L_2) = \Gamma(L_3)$	Expt.; Auger; free atom	S. Aksela, J. Väyrynen, and H. Aksela, *Phys. Rev. Lett.* 33, 999 (1974).
31 Ga	$\omega_K = 0.529(2)$	Expt.	A. Moljk, *Atlanta Conf. Proc.* (1973)*, p. 116.
32 Ge	$\omega_K = 0.570(3)$		
33 As	$\omega_K = 0.588(6)$		
32 Ge	$\omega_K = 0.561(15)$	Expt.	W. Hartl and J. W. Hammer, *Z. Physik*, A279, 135 (1976).
33 As	$\omega_K = 0.589(27)$	Expt.; AsH_3	W. M. Chew, J. C. McGeorge, and R. W. Fink, *Atlanta Conf. Proc.* (1973)*, p. 197
25-43	ω_K	Comparison between Expt. and Th.	
36 Kr	$\Gamma(L_2) = 1.3$ eV $\Gamma(L_3) = 1.2$ eV	Expt.; x-ray absorption	F. Wuilleumier, *J. Phys.* (Paris) 32, C4-88 (1971).
37-56	L x-ray spectra	Expt.; Coster-Kronig transition cut-offs near Z = 40 and 50	B. L. Doyle and S. M. Shafroth in *2nd Int. Conf. on Inner Shell Ionization Phenomena.* Abstract, Freiburg (1976), p. 211; and to be published (1978).
40 Zr	$\Gamma(L_1) = 4(1)$ eV $\Gamma(L_2) = 1.9(3)$ eV $\Gamma(L_3) = 1.6(3)$ eV	Expt.; semi-empirical deduced from x-ray line widths and spectral features	M. O. Krause, F. Wuilleumier, and C. W. Nestor, Jr., *Phys. Rev.* A6, 871 (1972).
41 Nb	$\Gamma(L\beta_3) = 10.5(5)$ eV; $\Gamma(L\beta_4) = 11$-13 eV $\Gamma(L\gamma_1) = 7$ eV	Expt.; x-ray lines	M. K. Bahl and A. S. Koster, *J. Phys.* C. 8, 1776 (1975).
47 Ag	$\Gamma(L_1) \approx 3.9$ eV	Semi-empirical; deduced from x-ray spectrum	M. H. Chen, B. Crasemann, M. Aayagi and H. Mark, *Phys. Rev.* A15, 2312 (1977).
47 Ag	$\omega_K = 0.834(17)$	Expt.	B. Fischer and K. W. Hoffman, *Z. Physik* A277,317 (1976).
51 Sb	$\omega_K = 0.868(14)$		
47 Ag	$\omega_1 = 0.034(3)$ $\omega_2 = 0.051(5)$; $\omega_3 = 0.035(4)$	Expt.	B. Budick and S. Derman, *Phys. Rev. Lett.* 29, 1055 (1972).
52 Te	$\omega_1 = 0.062(6)$ $\omega_2 = 0.071(7)$ $\omega_3 = 0.056(6)$		
50 Sn	$\omega_K = 0.857(10)$	Expt.	M. Hribar, A. Kodre, J. Pahor, and V. Stare, *Z. Physik* A 275, 323 (1975).
50-100	ω_3; ω_2; $f_{2,3}$	Compilation and comparison between Expt. and Th.	J. C. McGeorge, *Atlanta Conf. Proc.* (1973)*, p. 175
51 Sb	$\omega_K = 0.873(10)$	Expt.	M. Hribar, A. Kodre, and J. Pahor, *Z. Physik* A272, 413 (1975).
54 Xe	$\omega_K = 0.889(10)$	Expt.	M. Hribar, A. Kodre, and J. Pahor, *Z. Physik* A280, 227 (1977)
54 Xe	$\omega_3 = 0.099(2)$ $v_1 = 0.09(3)$ $v_2 = 0.106(7)$	Expt.	M. Hribar, A. Kodre, and J. Pahor, *Physica* 92C, 143 (1977).
57 La	$\omega_2 = 0.112(9)$; $\omega_3 = 0.092(8)$ $f_{2,3} = 0.21(2)$	Expt.	D. G. Douglas, *Can. J. Phys.* 51, 1519 (1973).
58-74	Γ (L x rays)	Expt.	S. I. Salem and P. L. Lee, *Phys. Rev.* A10, 2033 (1974).
63 Eu	$\omega_1 = 0.06(2)$; $f_{1,2} = 0.26(10)$ $f_{1,3} = 0.27(3)$ $v_1 = 0.138(7)$	Expt.	V. R. Veluri and P. V. Rao, *Z. Physik* A280, 317 (1977).
63 Eu	$f_{2,3} = 0.172(15)$	Expt.	M. K. Zalutsky and E. S. Macias, *Phys. Rev.* A11, 71 (1975).

APPENDIX. Reference list – continued

Listing comprises work subsequent to the reviews by Bambynek, *et al.* (1972), Burhop and Assad (1972) and Sevier (1972). Cut-off date October 1977.

Z Element	Data reported	Notes Expt.: Experiment Th.: Theory	Reference
64 Gd	$\omega_2 = 0.182(8)$ $\omega_3 = 0.187(6)$ $f_{2,3} = 0.223(11)$	Expt.	D. G. Douglas, *Can. J. Phys.* **50**, 1697 (1972).
67 Ho 69 Tm	$f_{2,3} = 0.143(10)$ $f_{2,3} = 0.148(7)$	Expt.	D. G. Douglas, *Can. J. Phys.* **54**, 1124 (1976).
70 Yb	$\omega_1 = 0.126(10)$; $f_{1,2} = 0.16(3)$; $f_{1,3} = 0.297(20)$	Expt.	L. A. McNelles, J. L. Campbell, J. S. Geiger, R. L. Graham, and L. S. Merritt, *Can. J. Phys.* **53**, 1349 (1975).
63 Eu 65 Tb 73 Ta 80 Hg 81 Tl	$f_{2,3} = 0.129(19)$ $f_{2,3} = 0.130(11)$ $f_{2,3} = 0.125(8)$ $f_{2,3} = 0.134(11)$ $f_{2,3} = 0.128(8)$ $f_{2,3} = 0.113(11)$ $\omega_2 = 0.239(7)$; $f_{2,3} = 0.130(10)$; $\nu_1 = 0.235(8)$ $\omega_3 = 0.220(7)$; $\nu_2 = 0.267(8)$	Expt.; compilation of previous data for $f_{2,3}$	V. R. Veluri, R. E. Wood, J. M. Palms and V. P. Rao, *J. Phys.* B7, 1486 (1974).
73 Ta	$\omega_3 = 0.235(18)$; $\nu_1 = 0.271(25)$	Expt.; on yields in L double-hole configuration.	J. L. Campbell, L. A. McNelles, J. S. Geiger, L. S. Merritt and R. L. Graham, *Can. J. Phys.* **55**, 868 (1977).
74 W	$\omega_1 = 0.106(23)$ $f_{1,2} = 0.260(63)$	Expt.	L. Salgueiro, M. T. Ramos, M. L. Escrivao, M. C. Martins, and J. G. Ferreira, *J. Phys.* B7, 342 (1974).
75 Re	$\omega_1 = 0.095(20)$ $f_{1,2} = 0.286(70)$		
77 Ir	$\omega_1 = 0.096(20)$ $f_{1,2} = 0.157(35)$		
79 Au	$\omega_1 = 0.098(20)$ $f_{1,2} = 0.207(51)$		
90 Th	$\omega_1 = 0.108(22)$ $f_{1,2} = 0.086(20)$		
76 Os	$\omega_2 = 0.300(22)$ $\omega_3 = 0.301(20)$ $f_{2,3} = 0.106(23)$	Expt.	S. Mohan, W. D. Schmidt-Ott, J. C. McGeorge and R. W. Fink, *Atlanta Conf. Proc.* (1973)*, p. 244.
78 Pt	$\omega_2 = 0.318(22)$ $\omega_3 = 0.309(20)$ $f_{2,3} = 0.126(21)$		
78 Pt 82 Pb 92 U	$\omega_K = 0.967(8)$ $\omega_K = 0.972(8)$ $\omega_K = 0.970(5)$	Expt.	J. S. Hansen, J. C. McGeorge, R. W. Fink, R. E. Wood, P. V. Rao, and J. M. Palms, *Z. Physik* **249**, 373 (1972).
80 Hg 81 Tl 82 Pb 92 U	$f_{2,3} = 0.123(12)$ $f_{2,3} = 0.109(11)$ $f_{2,3} = 0.105(11)$ $f_{2,3} = 0.146(18)$	Expt.	D. W. Nix and R. W. Fink, *Z. Physik* A273, 305 (1975).
63–96	$f_{2,3}$	Selected best values	
82 Pb	$f_{2,3} = 0.156(10)$	Expt.	R. E. Wood, J. M. Palms, P. V. Rao, *Phys. Rev.* A5, 11 (1972).
83 Bi	$\omega_2 = 0.35(3)$ $f_{2,3} = 0.18(7)$ $a_2 = 0.46(8)$ $\omega_3 = 0.33(2)$ $a_3 = 0.67(2)$ $\nu_2 = 0.41(3)$	Expt.	A. Maio, J. P. Ribeiro, A. Barroso, and F. B. Gil, *J. Phys.* B8, 1216 (1975).
83 Bi 93 Np	$\omega_1 = 0.118(11)$ $\omega_1 = 0.196(20)$ $f_{1,3} = 0.014(3)$	Expt.	M. Weksler and A. G. de Pinho, *Rev. Bras. de Fisica*, 3, 291 (1973).
86 Rn	$\omega_2 = 0.459(25)$ $\omega_3 = 0.384(20)$ $f_{2,3} = 0.105(11)$ $\nu_2 = 0.498(28)$	Expt.	J. C. McGeorge, D. W. Nix and R. W. Fink, *J. Phys.* B6, 573 (1973).

APPENDIX. Reference list – continued

Listing comprises work subsequent to the reviews by Bambynek, *et al.* (1972), Burhop and Assad (1972) and Sevier (1972). Cut-off date October 1977.

Z Element	Data reported	Notes Expt.: Experiment Th.: Theory	Reference
88 Ra	$\omega_2 = 0.493(30)$ $\omega_3 = 0.408(27)$ $f_{2,3} = 0.053(26)$ $\nu_2 = 0.516(36)$		
94 Pu	$\omega_2 = 0.513(22)$ $\omega_3 = 0.509(29)$ $f_{2,3} = 0.226(16)$ $\nu_2 = 0.627(36)$		
96 Cm	$f_{2,3} = 0.188(10)$		
88 Ra	$\omega_2 = 0.415(27)$ $f_{2,3} = 0.01(7)$ $a_2 = 0.571(84)$	Expt.	F. B. Gil, A. Barroso, J. C. Soares, and J. G. Ferreira, *Phys. Rev.* A5, 536 (1972).
92 U	$\omega_2 = 0.423(23)$ $f_{2,3} = 0.07(5)$ $a_2 = 0.522(56)$		
88 Ra	$\omega_2 = 0.498(27)$ $\omega_3 = 0.438(22)$ $f_{2,3} = 0.102(6)$	Expt.	J. L. Campbell, L. A. McNelles, J. S. Geiger, R. L. Graham and J. S. Merritt, *Can. J. Phys.* 52, 488 (1974).
94 Pu	$\omega_2 = 0.485(26)$ $\omega_3 = 0.484(17)$ $f_{2,3} = 0.229(4)$		
90 Th	$\omega_2 = 0.44(3)$	Expt.	J. G. Ferreira, J. C. Soares, A. Barroso, and F. B. Gil, *J. Phys.* A4, 679 (1971).
92 U	$\omega_2 = 0.560(33)$ $f_{2,3} = 0.147(10)$ $\omega_3 = 0.481(29)$ $\nu_1 = 0.54(4)$ $\nu_2 = 0.630(36)$	Expt.	J. C. McGeorge, D. W. Nix, and R. W. Fink, *Z. Physik*, 255, 335 (1972)
92 U 94 Pu	$f_{2,3} \approx 0.14$ $f_{2,3} = 0.24$	Expt.; test of onset of Coster-Kronig transitions near Z = 92	K. R. Baker, F. Tolea, R. W. Fink, and J. J. Pinajian, *Z. Physik* 270, 9 (1974).
94 Pu	$\omega_2 = 0.42(2)$ $f_{2,3} = 0.21(8)$ $a_2 = 0.37(8)$	Expt.	J. Byrne, R. J. D. Beattie, S. Benda, and J. Collingwood, *J. Phys.* B3, 1166 (1970).
93 Np 94 Pu 96 Cm 98 Cf 99 Es	$\omega_K = 0.971(5)$ $\omega_K = 0.973(5)$ $\omega_K = 0.972(7)$ $\omega_K = 0.972(5)$ $\omega_K = 0.971(5)$	Expt.	I. Ahmad, R. K. Sjoblom, *US-ERDA CONF-760539* (1976), p. 249
94 Pu 96 Cm	$f_{2,3} = 0.233(15)$ $f_{2,3} = 0.226(17)$	Expt.	M. R. Zalutsky and E. S. Macias, *Phys. Rev.* A11, 71 (1975).
95 Am 98 Cf 100 Fm	$f_{1,2} = 0.16(3)$ $f_{1,3} = 0.63(7)$ $f_{2,3} = 0.18(4)$	Expt. (preliminary); data are averages for indicated elements	M. S. Freedman and F. T. Porter, *Atlanta Conf. Proc.* (1973)*, p. 680.
96 Cm	$\omega_1 = 0.25(6)$ $f_{1,2} \leq 0.10$ $f_{1,3} = 0.69(8)$ $f_{1,3} = 0.015(4)$	Expt.	J. C. McGeorge and R. W. Fink, *Z. Physik.* 250, 293 (1972).
96 Cm	$f_{2,3} = 0.209(22)$	Expt.	D. W. Nix and R. W. Fink, *Z. Physik* A278, 234 (1976).
98 Cf	$\omega_K = 0.976(5)$	Expt.	M. S. Freedman, I. Ahmad, F. T. Porter, R. K. Sjoblom, R. F. Barnes, J. Lerner, and P. R. Fields, *Phys. Rev.* C15, 760 (1977).

**Proc. Intern. Conf. on Inner Shell Ionization Phenomena and Future Applications.* Edited by R. W. Fink, S. T. Manson, J. M. Palms, and P. Venugopala Rao. US-AEC CONF-720404 (1973) available from National Information Service, U.S. Department of Commerce, Springfield, Va. 22151, USA.